ASSESSING THE ANORTHOSITE COMPOSITION AT SITES OF PUREST ANORTHOSITE SPECTRAL IDENTIFICATION USING LROC NARROW ANGLE CAMERA PHOTOMETRY. E. Culley[1], B. L. Jolliff[1], R. N. Watkins[2,3], and T. Hahn[4], [1]Department of Earth and Planetary Sciences and the McDonnell Center for the Space Sciences, Washington University in St. Louis, Box 1169, 1 Brookings Drive, Saint Louis, MO 63130, USA, [2]Planetary Science Institute, 1700 E. Fort Lowell, Suite 106, Tucson, AZ 85719, USA. [3]Arctic Slope Regional Corporation Federal Holding Company, 7000 Muirkirk Meadows Drive, Suite 100, Beltsville, MD 20705, USA. [4]School of Earth and Space Exploration, Arizona State University, PO Box 876004, Tempe, AZ 85287, USA. (eculley@wustl.edu)

Introduction: The primary lunar crust was formed during solidification of an ancient lunar magma ocean (LMO) [1,2]. After 75-80% of the LMO had solidified, plagioclase began to crystallize, accumulating upwards to form a feldspathic flotation crust [e.g. 3-5]. The extent to which denser mafic residual melt was expelled during accumulation of plagioclase and the end of solidification in the magma ocean is still debated. Apollo samples include specimens of highly pure anorthosite such as 4.6 kg ferroan anorthosite 60015 [6] (≥98% plagioclase, i.e., "purest anorthosite" or "PAN" [7]). Such a high percentage of plagioclase indicates extremely efficient separation of buoyantly accumulated plagioclase and trapped mafic material. Additionally, spectral analyses from the Moon Minerology Mapper [8] and SELENE [7] detect the presence of the 1.25-micron absorption feature indicative of plagioclase. This spectral feature is readily overwhelmed by more mafic mineral signatures, indicating that the detection of this feature is strong evidence for the presence of PAN (≥98% plagioclase) or "pure anorthosite" (≥96% plagioclase) [9].

This study uses single scattering albedo and composition, represented by FeO content, to determine the amount of plagioclase present in the regolith in areas where spectral studies indicate the presence of PAN. We focus on uplift structures (basin ring structures and central peaks) because these positive relief features undergo continuous degradation and exposure of uplifted crustal material. Determining wide extents of surficial PAN would indicate that ancient plagioclase separation was indeed extremely efficient, squeezing nearly all trapped melt out of the exposed primary anorthositic crust. On the other hand, if spectrally detected PAN is exceptional where observed, such a distribution may provide evidence that PAN occurs at a spatially limited scale, e.g., outcrop scale, and that trapped melt components were not effectively removed from the entire crust, at least as reflected in surface exposures.

Methods and Data: We used photometric analysis of Narrow Angle Camera (NAC) images from the Lunar Reconnaissance Orbiter Camera (LROC) to investigate compositional characteristics of regolith in areas where hyperspectral data indicate plagioclase and a near absence of mafic silicates. We determine single scattering albedo using Hapke photometric modeling [10,11], combined with digital terrain models (DTM) to account for local incidence and emission angles at every pixel (5 mpp) (e.g. [12]).

Results presented previously [13,14] show that single scattering albedo relates linearly to composition, using FeO content as a proxy. Figure 1 shows the expected single scattering albedo for anorthosite with varying amounts of plagioclase based on FeO content. PAN contains less than 0.5 wt% FeO and thus plots near the intercept, around w = 0.54-0.55. Additionally, we determined that fresh, immature material typically has a higher single scattering albedo than mature regolith and deviates from the linear relationship [14]. Thus, in this study, we focus on areas where OMAT < 0.21 (maturity index computed from data collected by SELENE) [15].

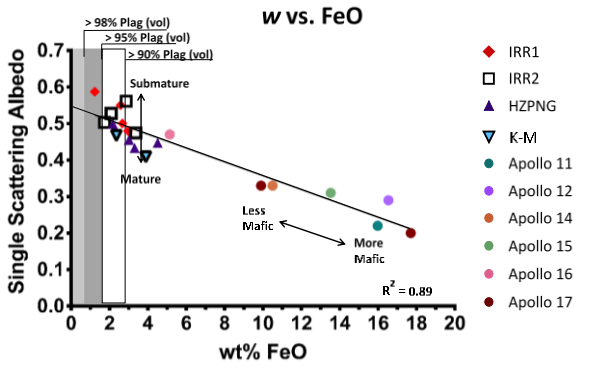

Figure 1. Relationship between SSA and wt% FeO established for Apollo landing site soils [12)] and PAN location soils [13]. Scatter above the correlation line is primarily a function of maturity, whereas location along the line is a function of FeO content or mafic mineralogy. The shaded areas highlight the SSA and FeO content ranged for anorthosites with 90%, 95%, and 98% plagioclase.

Results and Discussion: In this study, we compare the Inner Rook Ring of Orientale Basin (IRR1 and IRR2), the inner ring of Hertzsprung Basin, crater Korolev-M, and a region of highlands northeast of Nectaris Basin. In each region, we determined the single scattering albedo of regolith over segments of highest topography, i.e., uplifted material. Figure 2 shows the single scattering albedo for the study locations in Orientale and near Nectaris, highlighting the areas of highest topography, referred to hereafter as the central massif. In this figure, the dark blue and purple show material more mafic than anorthosite. Upon inspection, both IRR sites contain significantly more anorthositic material than the Nectaris highlands site.

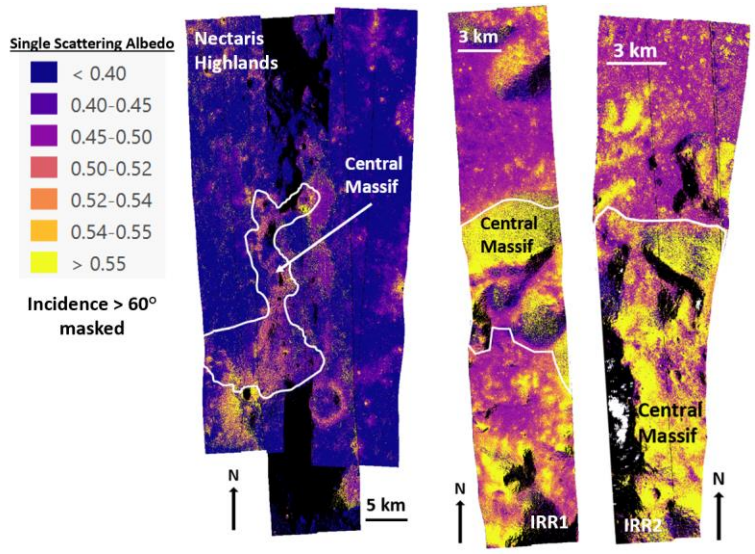

Figure 2. Single Scattering Albedo Parameter Maps for the Nectaris Highlands and Orientale (IRR1 and IRR2) regions considered in this study. SSA values of anorthosite with 90% plagioclase: w = 0.50-0.52; 95%: w = 0.52-0.54; 98%: w = 0.54-0.55. SSA values greater than 0.55 likely indicate high slope or immature material. White outlines show Central Massif morphological units. Pixels that were recorded with incidence > 60° are masked.

Focusing on only the central massifs in each region, Figure 3 shows the single scattering albedo distribution across the two locations. These distributions show that the average single scattering albedo in the central massif of the Inner Rook Ring sites is in the range expected for anorthosite, specifically, pure anorthosite (>96% plagioclase). The Nectaris region, on the other hand, has an average single scattering albedo and FeO content (determine by SELENE) more representative of regolith that has been mixed with mafic materials and contains 70-85% plagioclase. The Hertzsprung and Korolev-M sites analyzed show similar trends as the Nectaris region. In all three areas, regolith with single scattering albedo in the range expected for PAN only exists in very localized patches, or in immature areas, such as near small craters or on steep slopes where mass wasting occurs. Only the Inner Rook Ring sites of Orientale show evidence of extensive PAN and pure anorthositic regolith.

Conclusions: Our studies of the single scattering albedo in areas where spectral analysis has indicated the presence of highly pure anorthosite do not generally indicate widespread layers of PAN. Rather, most areas have single scattering albedo values and FeO content consistent with regolith developed from anorthosite with plagioclase <96%. This lower plagioclase content supports a primary crust with moderate proportions of trapped melt remaining after lunar magma ocean solidification or suggests that the surface material is well mixed with a more mafic suite.

Acknowledgments: We thank NASA for support of the LRO extended mission and for the hard work of the LRO and LROC Operations Teams. Additional thanks to the LROC Photometry Group. We appreciate colleagues at ASU for production of NAC DTMs.

References: [1] Smith J. et al. (1970) *Apollo 11 LSC*, 897-925. [2] Wood J. et al. (1970) *Apollo 11 LSC*, 965-988. [3] Longhi J. (1977) *JGR* **108**, 5083. [4] Rapp J. and Draper D. (2018) *MPS* **53**, 1432-1445. [5] Charlier B. et al. (2018) *GCA* **234**, 50-69. [6] Ryder, G., and Norman (1980) Catalog of Apollo 16 Rocks. [7] Ohtake, M., et al. (2009) *Nature* **461**, 236-241. [8] Donaldson-Hanna K. et al. (2014) *JGR* **119,** 1516-1545. [9] Cheek L. et al. (2013) *JGR*, **118**, 1805-1820. [10] Hapke B. (2012a) *Icarus*, **221** (2), 1079-1083. [11] Hapke B. (2012b) *Theory of Reflectance and Emittance Spectroscopy* (2nd Ed). [12] Clegg-Watkins, R. et al. (2017) *Icarus* **285**, 169-184. [13] Schonwald A. et al. (2019) *LPSC* **50**, #1239. [14] Jolliff B. et al. (2020) *LPSC* **51**, #2362. [15] Lucey P. et al. (2000) *JGR* **105**, 20377-20386.

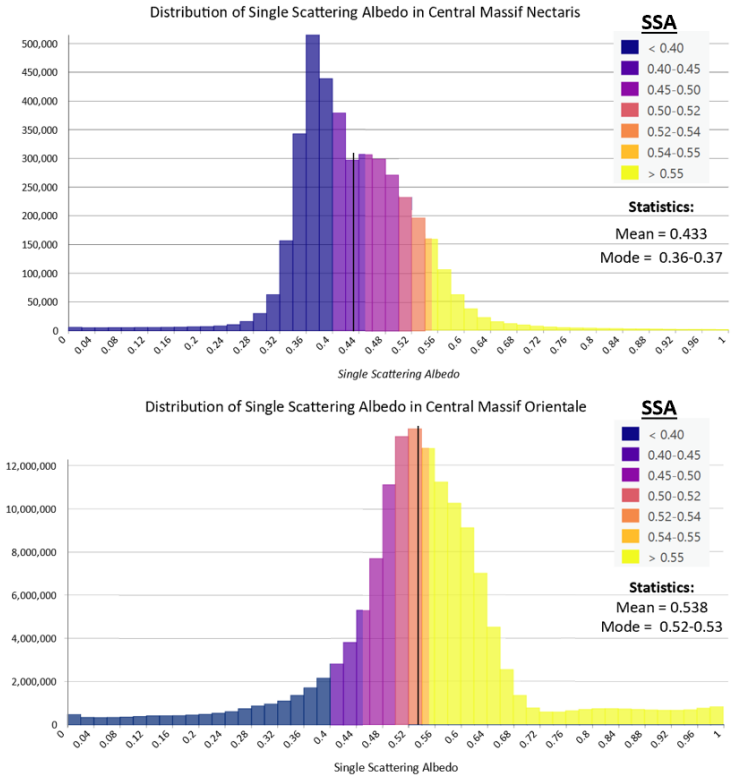

Figure 3. Distribution of SSA (w) values in central massif regions for the Nectaris Highlands and Orientale (IRR1 and IRR2) sites. Central massif regions and color gradient correspond to those outlined in Figure 2. The black line in each histogram represents the mean of that distribution.